

Electron-energy-loss spectrum of the cuprate superconductors

D. L. Mills

Department of Physics, University of California, Irvine, California 92717

R. B. Phelps and L. L. Kesmodel

Department of Physics, Indiana University, Bloomington, Indiana 47405

(Received 16 March 1994)

We present a theoretical description of the near-specular (dipole) electron-energy-loss spectrum of a superlattice constructed from anisotropic dielectric layers, as a model of the superconducting copper-oxide-based materials. The theory is applied to a description of recent data taken on the Bi 2:2:1:2 compound. We find that parameters deduced from the electron loss spectrum are compatible with infrared reflectivity data. Manifestations of the superconducting energy gap are not evident in the new data.

I. INTRODUCTION

High-resolution electron-energy-loss spectroscopy can be used to probe a diverse array of elementary excitations on crystal surfaces. The technique has been applied in numerous instances where microscopically thin conducting layers are present on the surface.¹ Such data, when taken in the near-specular scattering geometry where the electric dipole mechanism is operative, can be analyzed quantitatively through use of the basic theory² and its various extensions.³ By this means, one may extract information on the conductivity of thin layers on or near the surface, and analyze the influence of such layers on the intensity of dipole-active surface vibrations.

In the recent literature, the method has been applied to the superconducting copper-oxide-based materials.⁴ It has been argued by these authors that a signature of the superconducting energy gap appears in the electron-energy-loss spectrum.

However, a new series of experimental studies has been completed by two of us and our collaborators, which raises serious questions about the earlier data.⁵ The new experiments show strong phonon peaks in the energy-loss regime where the gap structure was found earlier. In addition, the background, whose origin, as we shall argue here, is provided by electronic fluctuations in the CuO₂ layers, is roughly two orders of magnitude stronger in the new experiments than in the earlier data. It is argued in Ref. 5 that the very low backgrounds reported earlier⁴ are evidence that, in the experiments, the substrate had acquired a net negative charge after its exposure to the electron beam. In this circumstance, the beam electrons are repelled as they approach the sample, and never actually reflect from the surface. Very high backgrounds, strong phonon peaks, and the absence of an energy gap in the loss spectrum have been reported also by Franchy, Decker, Masuch, and Ibach, in their study of YBa₂Cu₃O_{7-x} by near-specular electron loss spectroscopy.⁶

In this paper, we present a theory of the electron loss spectrum in the dipole regime, for an anisotropic layered structure such as the high- T_c materials. We apply this to

an analysis of the data on the Bi₂Sr₂CaCu₂O₈ (Bi 2:2:1:2) compounds reported in Ref. 5, and also explore a number of related questions. We shall see that the electron loss data provide material parameters which may be used to describe the infrared reflectivity of these samples. The agreement we obtain with the data of Zibold *et al.*⁷ by this means is quite satisfactory, save for the fact that one mode observed in the infrared spectrum is not resolved in the electron loss measurements. The fact that the electron loss and infrared data are accounted for nicely within a single picture provides strong support for the argument that the data reported in Ref. 5 indeed represent the intrinsic loss spectrum of the uncharged surface.

As remarked earlier, the experiments explore electrons which suffer only very small angle deflections in the inelastic scattering event, and thus emerge from the surface very close to the specular beam. The angular variation of the strength of the inelastic losses contains a strong, near-specular peak that is the subject of study here. This feature has its physical origin in electrons scattered inelastically from long-ranged electric field fluctuations in the vacuum above the crystal produced by the vibrational and electronic fluctuations near the surface. Such long-ranged Coulomb fields produce intense small-angle scatterings. Through use of an appropriate version of the fluctuation-dissipation theorem, one may relate the near-specular (dipole) loss cross section to the frequency-dependent dielectric response functions that characterize the constituents of the substrate.^{2,3}

The present analysis is based on an extension of the theory of dipole scattering from dielectric superlattices, as described initially by Camley and Mills,⁸ and later extended to apply to a structure whose outermost layer may differ in thickness and physical properties from those in the underlying superlattice.⁹ These previous treatments assume each of these layers may be described by an isotropic, frequency-dependent dielectric function which, of course, is complex. We provide the extension of the formulas in Ref. 9 to the case where each layer is a uniaxial dielectric. In our application to the high- T_c materials, we model the CuO₂ layers by endowing them with a Drude conductivity parallel to the surfaces, and the insu-

lating regions as dielectric layers with suitable infrared-active vibrational excitations. The analysis in the paper by Persson and Demuth⁴ is based on a similar picture. However, their paper displays and employs special limiting forms of the general description, at various points.

The organization of this paper is as follows. Section II presents the extension of the dipole loss theory to the multilayered, anisotropic dielectric. Section III describes application of the theory to analyze the data on the Bi 2:2:1:2 compounds, along with a discussion of the infrared reflectivity. Conclusions and final remarks are found in Sec. IV.

II. THE THEORY

The model we consider is described by Fig. 1. We have a semi-infinite superlattice, fabricated from films of two materials, *A* and *B*. The structure has an outer layer of material *C*, whose thickness and properties may differ from the layers of the underlying material. We have in mind identifying the *B* layers with the highly conducting CuO₂ planes, and the *A* layers with the insulating regions between the CuO₂ planes. When we apply the model to the Bi 2:2:1:2 structures, we assume that cleavage of the crystal severs the bonds between the two BiO planes, producing an outer layer thinner than the interior insulating layers.

Each of the dielectric films is described by an anisotropic dielectric tensor of uniaxial character. The dielectric response perpendicular to the surfaces of each film is $\epsilon_{\perp}(\omega)$, and that parallel to the surfaces is $\epsilon_{\parallel}(\omega)$. The conducting layers will be modeled by adding the contribution $4\pi i\sigma_{\parallel}(\omega)/\omega$ to $\epsilon_{\parallel}(\omega)$, while $\epsilon_{\perp}(\omega)$ for these layers is assumed real and independent of frequency. The dipole-active vibrations evident in the electron-energy-loss or infrared spectra are introduced by adding the appropriate resonant terms to the dielectric constants of the insulating spacer layers. We will discuss these choices in more detail in Sec. III. Here it will suffice to simply endow each film with the complex, frequency-dependent dielectric functions, as just described.

In the near-specular dipole regime, the electron loss spectrum is described as follows.² Let I_0 be the intensity of the elastic beam, specularly reflected from the surface. Of course, I_0 depends on both the beam energy and the angle of incidence. Then the number of electrons which emerge from the surface with energy loss between $\hbar\omega$ and $\hbar(\omega + d\omega)$ may be written $I_0 P(\omega) d\omega$, where $P(\omega)$ depends on frequency-dependent dielectric functions of the constituents of the substrate, in addition to the beam energy and angle of incidence. Our interest here is in $P(\omega)$. We note there are instances where this simple picture of dipole scattering breaks down,¹⁰ but such questions are of no concern in the experiments of interest here.

For the model illustrated in Fig. 1 it is quite straightforward to derive the form of $P(\omega)$, by following a pro-

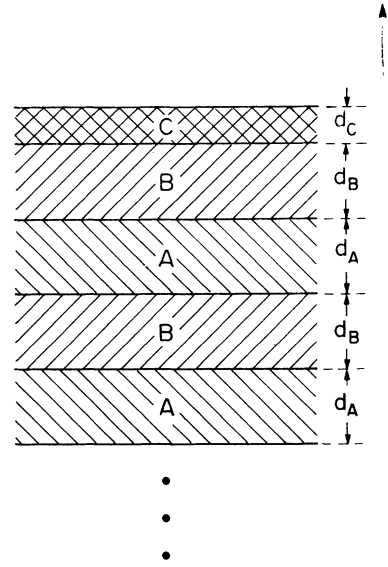


FIG. 1. The model structure considered in this paper. We have a semi-infinite superlattice fabricated from layers of material *B* and material *A*, capped by a layer of material *C*. Each film is described by its complex, uniaxial dielectric tensor with elements $\epsilon_{\perp}(\omega)$ and $\epsilon_{\parallel}(\omega)$ for response perpendicular and parallel to the surfaces, respectively.

cedure very similar to that used in Ref. 8 or 9. As a consequence, we shall only quote the final result.

The dipole loss probability $P(\omega)$ has a form identical to that given in Eq. (3.22) of the paper by Camley and Mills.⁸ We require the form of the loss function $\text{Im}[R(Q_{\parallel}, \omega)]$ which appears in the integrand. This may be written in a form similar in structure to Eq. (3.16) of Ref. 8. We have here

$$\begin{aligned} \text{Im}[R(Q_{\parallel}, \omega)] \\ = \text{Im} \left[\frac{-1}{1 + \bar{\epsilon}_C(\omega)[1 - F(Q_{\parallel}, \omega)]/[1 + F(Q_{\parallel}, \omega)]} \right], \end{aligned} \quad (1)$$

where

$$\bar{\epsilon}_C(\omega) = [\epsilon_{\parallel}^C(\omega)\epsilon_{\perp}^C(\omega)]^{1/2} \quad (2)$$

is the geometrical mean of the two dielectric-tensor elements of the outermost layer. We shall express quantities below in terms of $\bar{\epsilon}_B(\omega)$ and $\bar{\epsilon}_A(\omega)$, defined similarly. We also encounter quantities such as

$$Q_{\parallel}^C = \left[\frac{\epsilon_{\parallel}^C(\omega)}{\epsilon_{\perp}^C(\omega)} \right]^{1/2} Q_{\parallel}. \quad (3)$$

Then

$$F(Q_{\parallel}, \omega) = \exp[-2Q_{\parallel}^C d_C] \left[\frac{[\bar{\epsilon}_C(\omega) + \bar{\epsilon}_B(\omega)]G(Q_{\parallel}, \omega) + [\bar{\epsilon}_C(\omega) - \bar{\epsilon}_B(\omega)]}{[\bar{\epsilon}_C(\omega) - \bar{\epsilon}_B(\omega)]G(Q_{\parallel}, \omega) + [\bar{\epsilon}_C(\omega) + \bar{\epsilon}_B(\omega)]} \right], \quad (4)$$

where

$$G(Q_{\parallel}, \omega) = \frac{\tilde{\epsilon}_B(\omega) + \tilde{\epsilon}_A(\omega)}{\tilde{\epsilon}_B(\omega) - \tilde{\epsilon}_A(\omega)} \times \frac{\exp[-Q_{\parallel}^B d_B] - \exp[-\beta d + Q_{\parallel}^A d_A]}{\exp[+Q_{\parallel}^B d_B] - \exp[-\beta d + Q_{\parallel}^A d_A]} \quad (5)$$

In Eq. (5), $d = d_A + d_B$ is the thickness of the superlattice unit cell, and β is found by solving

$$\begin{aligned} \cosh[\beta d] &= \cosh[Q_{\parallel}^B d_B] \cosh[Q_{\parallel}^A d_A] \\ &+ \frac{1}{2} \left[\frac{\tilde{\epsilon}_A(\omega)}{\tilde{\epsilon}_B(\omega)} + \frac{\tilde{\epsilon}_B(\omega)}{\tilde{\epsilon}_A(\omega)} \right] \\ &\times \sinh[Q_{\parallel}^B d_B] \sinh[Q_{\parallel}^A d_A]. \end{aligned} \quad (6)$$

It is straightforward to evaluate $P(\omega)$ from the above expressions, for any specific model of the dielectric response of the constituents. However, these expressions are indeed cumbersome, and as a consequence they offer little insight into the key features which influence the loss spectrum. We conclude this section with comments on special limiting cases.

First, suppose that we have a simple semi-infinite dielectric substrate, whose dielectric response perpendicular to the surface may differ from that parallel to it. To describe this, we let $d_C \rightarrow \infty$, and drop the superscript C on $\epsilon_{\parallel}^C(\omega)$ and $\epsilon_{\perp}^C(\omega)$ to find

$$R(Q_{\parallel}, \omega) = \frac{-1}{1 + [\epsilon_{\parallel}(\omega)\epsilon_{\perp}(\omega)]^{1/2}}, \quad (7)$$

an expression that appears also in the paper on the high- T_c materials by Persson and Demuth.⁴

Suppose the substrate is a simple isotropic highly conducting material, such as copper metal. Then

$$\epsilon_{\parallel}(\omega) = \epsilon_{\perp}(\omega) = \epsilon_{\infty} + 4\pi i \sigma(\omega) / \omega,$$

where ϵ_{∞} has its origin in interband transitions. In the infrared, the term involving $\sigma(\omega)$ dominates, and to excellent approximation, if $\sigma(\omega) = \sigma_1(\omega) + i\sigma_2(\omega)$,

$$\text{Im}[R(Q_{\parallel}, \omega)] \cong \frac{\omega}{4\pi} \rho_1(\omega), \quad (8)$$

where

$$\rho_1(\omega) = \frac{\sigma_1(\omega)}{\sigma_1^2(\omega) + \sigma_2^2(\omega)} \quad (9)$$

is the real part of the frequency-dependent resistivity.

The behavior and magnitude of $R(Q_{\parallel}, \omega)$ are very different than those displayed in Eq. (8), if the conductivity is highly anisotropic. With the cuprate materials in mind, suppose we consider a substrate with large parallel conductivity $\sigma_{\parallel}(\omega)$, so that $\epsilon_{\parallel}(\omega) \cong 4\pi i \sigma_{\parallel}(\omega) / \omega$, while $\epsilon_{\perp}(\omega) = \epsilon_{\perp}$ independent of frequency. This picture would be appropriate to a material with electrons confined to infinitesimally thin two-dimensional sheets parallel to the surface.

Then we have

$$\text{Im}[R(Q_{\parallel}, \omega)] = \frac{\omega^{1/2}}{2\sqrt{\pi\epsilon_{\perp}}} \text{Im} \left\{ \frac{+i}{\sqrt{\sigma_{\parallel}(\omega)}} \right\}. \quad (10)$$

We see that if ϵ_{\perp} assumes a value characteristic of a typical insulator, and the conductivities in Eqs. (8) and (10) are the same order of magnitude, the contribution to the loss spectrum from fluctuations of the conduction electrons is very much *larger* for the anisotropic materials. For Cu at room temperature, and $\hbar\omega \cong 100$ meV, one has $4\pi\sigma(\omega)/\omega \cong 10^4$, so the background for the isotropic material is roughly two orders of magnitude *smaller* than for a highly anisotropic material of the same conductivity confined to sheets parallel to the surface. The background signal levels are a central ingredient in the arguments advanced by Phelps and collaborators.⁵

In the papers by Lieber and co-workers,¹¹ it is argued that the free-carrier contribution to the loss spectrum of the cuprates is proportional to the real part of the resistivity $\rho_1(\omega)$. We see that, for very anisotropic materials such as the cuprates, this claim is incorrect, as is evident also from the earlier discussions by Persson and Demuth.⁴ We shall illustrate this point further with the numerical calculations reported below.

If we have highly conducting films of finite thickness present, then it is essential to utilize the full expression for $R(Q_{\parallel}, \omega)$. This point is illustrated by examining the form of $R(Q_{\parallel}, \omega)$ for the case where we have a single conducting layer placed over a semi-infinite dielectric substrate. Expressions derived earlier,³ generalized to the case where both media are anisotropic, are found by setting d_A to zero. We then have a film of material C on a semi-infinite substrate of material B . One has $G(Q_{\parallel}, \omega) \rightarrow 0$ here, so

$$F(Q_{\parallel}, \omega) = \exp[-2Q_{\parallel}^C d_C] \frac{\tilde{\epsilon}_C(\omega) - \tilde{\epsilon}_B(\omega)}{\tilde{\epsilon}_C(\omega) + \tilde{\epsilon}_B(\omega)} \quad (11)$$

suppose also that d_C is very small. We then keep the contributions to $(1-F)/(1+F)$ first order in d_C to find

$$R(Q_{\parallel}, \omega) \cong \frac{-1}{1 + [\epsilon_{\parallel}^B(\omega)\epsilon_{\perp}^B(\omega)]^{1/2} + \epsilon_{\parallel}^C(\omega)Q_{\parallel}d_C \{1 - [\tilde{\epsilon}_B(\omega)/\tilde{\epsilon}_C(\omega)]^2\}} \quad (12)$$

If the outermost layer has very high conductivity parallel to the surface, then even though $Q_{\parallel}d_C$ may be small compared to unity, the combination $\epsilon_{\parallel}(\omega)Q_{\parallel}d_C$ may be large. Consider some numbers. In electron-

energy-loss spectroscopy, $Q_{\parallel} \cong (\hbar\omega/2E_I)k_I$,¹² with $\hbar\omega$ the energy loss, and E_I, k_I the energy and wave vector of the incident electron. If $E_I \cong 3$ eV as in the experiments discussed below, and $\hbar\omega \cong 100$ meV, then $Q_{\parallel} \cong 1.6 \times 10^6$

cm^{-1} . If we have $d_C \cong 3 \text{ \AA}$, then $Q_{\parallel} d_C = 0.05 \ll 1$. But if the overlayer has the conductivity of Cu, we have seen already that $\epsilon_{\parallel}(\omega) \cong 10^4$. Quite clearly, the full dependence of the loss cross section on Q_{\parallel} must be retained. Even the first term in Q_{\parallel} , described by Eq. (12), is inadequate.

In earlier work by Dubois *et al.*,¹ the influence of microscopically thin Ag overlayers on the loss spectrum GaAs was studied. It was found that even a monolayer of Ag influenced the loss spectrum very substantially; the very strong surface optical phonon signal from this ionic material was screened out completely from such a very thin layer. The model derived from the form in Eq. (11) described these data very well.

One might think it possible that, since the superconducting cuprates have very thin conducting CuO_2 sheets separated by very thin insulating layers, the electron loss spectrum can be described by treating the substrate by effective-medium theory, wherein the structure is replaced by a semi-infinite dielectric described by average dielectric constants which characterize its response parallel and perpendicular to the surface. The above example shows that such a description is inappropriate. One must retain a full description of the microstructure of the substrate. We shall illustrate this point further in Sec. III, when we show the loss spectrum to be very sensitive to whether the outermost layer is insulating in nature, or consists of a conducting CuO_2 sheet. The data reported in Ref. 5 are compatible with only the first possibility, as we shall see.

III. A COMPARISON BETWEEN THEORY AND EXPERIMENT: THE CASE OF Bi 2:2:1:2

In this section, we apply the theory outlined in Sec. II to the analysis of electron-energy-loss data taken on the Bi 2:2:1:2 material in its superconducting state. We shall see that we can extract from these data a set of material parameters that also may be used to reproduce the infrared reflectivity data reported by Zibold and co-workers, as remarked earlier.⁷

The data that will be the focus of our attention are reproduced from Ref. 5 in Fig. 2. We see a quasielastic peak centered around zero energy loss, and then a rather intense background which falls off slowly with increasing energy loss. Upon the background are superimposed three vibrational loss peaks. We argue the background has its origin in fluctuations in the conduction electrons contained in the CuO_2 plane, i.e., in the particle-hole excitations of these structures.

We first comment on how one may extract absolute values for the loss function from such data. As remarked in Sec. II, the fraction of the electrons in the incident beam that suffer energy losses between $\hbar\omega$ and $\hbar(\omega + d\omega)$ is $I_0 P(\omega) d\omega$, where I_0 is the total number of electrons in the specular beam which reflect elastically from the surface. There is an energy spread in the incident beam, so a scan of the energies of the electrons in the specular beam produces the approximately Lorentzian feature centered about zero energy in Fig. 2. If $\delta\omega$ is the half width of the quasielastic beam at half maximum, the number of elec-

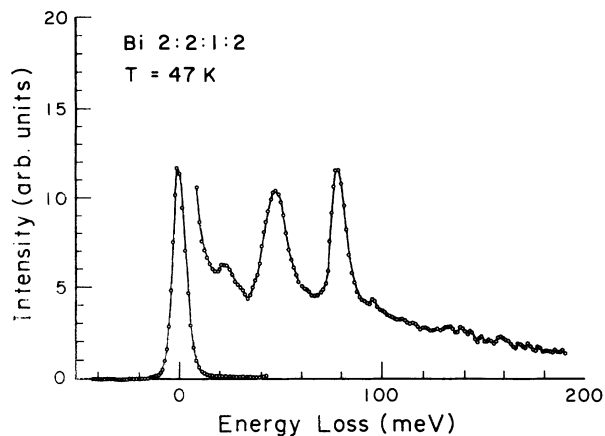


FIG. 2. The electron-energy-loss spectrum of Bi 2:2:1:2. The data are reproduced from Ref. 5. We see the quasielastic peak, and the portion of the loss spectrum which contains the vibrational losses is multiplied by a factor of 40.

trons found in the specular beam in the window $d\omega$ is $I_0 \{ \delta\omega / \pi [\omega^2 + (\delta\omega)^2] \} d\omega$. If we assume that scattered electrons are collected in bins of width $\Delta\omega$, the peak intensity I_m at $\omega=0$ in the specular beam is $I_M = I_0 \Delta\omega / \pi \delta\omega$. The number I_M and $\delta\omega$ may be extracted from Fig. 2. If $I_{\text{loss}}(\omega)$ is the strength of the loss spectrum in Fig. 2, then $I_{\text{loss}}(\omega) = I_0 P(\omega) \Delta\omega$, which gives $P(\omega) = I_{\text{loss}}(\omega) / [\pi \delta\omega I_M]$. From Fig. 2, we estimate $\delta\omega = 2 \text{ meV}$, while $I_M = 12 \text{ units}$. At 100 meV , $I_{\text{loss}}(\omega) \cong 0.1$, so we estimate $P(100 \text{ meV}) \cong 1.3 \times 10^{-3} \text{ meV}^{-1}$. We shall use this number as a means of assessing the conductivity of the layers.

For appropriate superlattice structures, we find that layer resistivities in the range $50\text{--}200 \mu\Omega \text{ cm}$ provide reasonable values for the background. The shape of the background is controlled, however, by the means of modeling the frequency dependence of the parallel conductivity of the layers, $\sigma_{\parallel}(\omega)$. We illustrate this in Fig. 3. Here we have a semi-infinite superlattice, with A layers insulating, and B layers endowed with a frequency-dependent metallic conductivity $\sigma_{\parallel}(\omega)$. For $\sigma_{\parallel}(\omega)$ we take the Drude form, where $\sigma_{\parallel}(\omega) = \sigma_0 / [1 - i\omega\tau_0]$, where for now both σ_0 and τ_0 are independent of frequency.

In Fig. 3(a), we show calculations of $P(\omega)$ for various choices of the relaxation time τ_0 . Once τ_0 is chosen, we adjust σ_0 so $P(\omega)$ assumes the value $1.3 \times 10^{-3} \text{ meV}^{-1}$ at a 100 meV loss, and then calculate the whole curve. Very short relaxation times are required for the theoretical curve to fall off substantially with increasing ω , as we move above 100 meV . If τ_0 is then chosen quite short, less than 10^{-15} s , then we also require quite a large value of the layer resistivity $\rho_0 = 1/\sigma_0$; we require layer resistivities above $400 \mu\Omega \text{ cm}$ to obtain a background similar to that in the data.

More reasonable parameters can provide an account of the background if we make the relaxation time τ depend on frequency. This is illustrated in Fig. 3(b), where we take $\sigma_{\parallel}(\omega) = \sigma_0 / [1 - i\omega\tau(\omega)]$, where $\tau(\omega) = \tau_0 / [1 + (\omega/\omega_0)^2]$. We have here the choice $\rho_0 = 1/\sigma_0 = 163 \mu\Omega \text{ cm}$, $\tau_0 = 10^{-14} \text{ sec}$, and $\omega_0 = 138 \text{ meV}$

to generate curve (2) in the figure. Of course, in the Drude model, $\sigma_0 = ne^2\tau/m$, so if τ is frequency dependent we should allow σ_0 to depend on frequency as well. We follow the arguments put forward by Webb, Sievers, and Mihalisin¹³ in their analysis of the infrared response of the heavy-fermion material CePd₃ by arguing that the frequency dependence of $\tau(\omega)$ and that of the quasiparticle effective mass compensate, rendering σ_0 frequency independent.

We must keep in mind that we are applying a simple phenomenology to a material whose underlying physics is understood incompletely. Thus we cannot claim that the parameters which emerge from the analysis are unique. We can and do argue, however, that the discussion just completed, along with that given in the remainder of the section, demonstrates that the energy-loss spectra reported in Ref. 5 can be described nicely by a reasonable and physically plausible set of parameters.

We now include the vibrational losses into the analysis. As we do so, we shall retain the form just described by

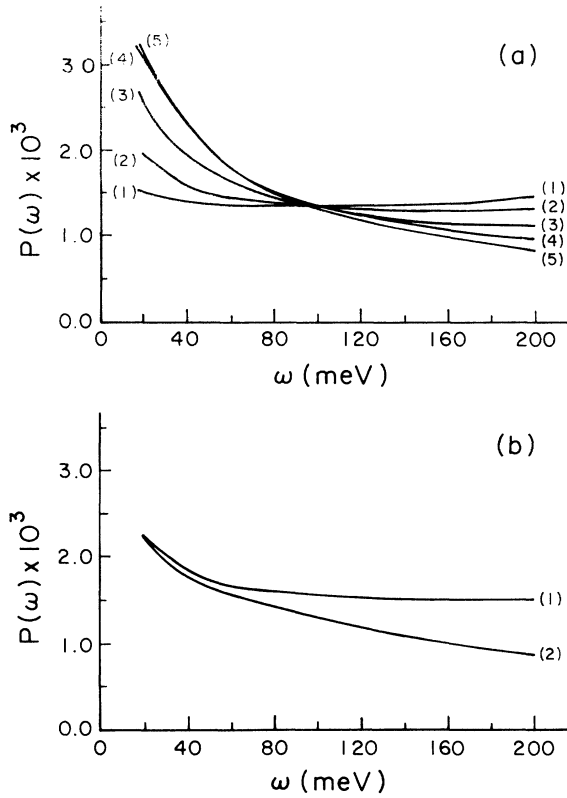


FIG. 3. The function $P(\omega)$, as a function of the loss energy, for various models of the conductivity. We have (a) $\sigma_{\parallel}(\omega) = \sigma_0 / (1 - i\omega\tau_0)$, with σ_0 and τ_0 independent of frequency, and the following choices of parameters: (1) $\rho_0 = 1/\sigma_0 = 43 \mu\Omega$ cm and $\tau_0 = 10^{-14}$ sec, (2) $\rho_0 = 121 \mu\Omega$ cm and $\tau_0 = 3.1 \times 10^{-14}$ sec, (3) $\rho_0 = 283 \mu\Omega$ cm and $\tau_0 = 3 \times 10^{-15}$ sec, (4) $\rho_0 = 425 \mu\Omega$ cm and $\tau_0 = 10^{-15}$ sec, and (5) $\rho_0 = 472 \mu\Omega$ cm and $\tau_0 = 10^{-16}$ sec. In (b) we have curves calculated for (1) σ_0 and τ_0 independent of frequency, with $\rho_0 = 1/\sigma_0 = 163 \mu\Omega$ cm, $\tau_0 = 10^{-14}$ sec, and (2) $\rho_0 = 1/\sigma_0 = 163 \mu\Omega$ cm independent of frequency, $\tau(\omega) = \tau_0 / (1 + [\omega/\omega_0]^2)$ where $\tau_0 = 10^{-14}$ sec, and $\hbar\omega_0 = 138$ meV.

$\tau(\omega)$ always, then adjust σ_0 to provide the value 1.3×10^{-3} for $P(\omega)$ at the energy loss of 100 meV.

The vibrational losses may be introduced simply by appending the appropriate resonant terms in the frequency-dependent dielectric functions. For instance, if we wish to simulate dipole-active vibrations in the insulating A layers, polarized perpendicular to their surfaces, we use for the dielectric function of the A layers

$$\epsilon_{\perp}^A(\omega) = \epsilon_{\perp}^A(\infty) + \sum_j \frac{A_j^2}{\omega_j^2 - \omega^2 - i\omega\gamma_j} \quad (13)$$

while ϵ_{\parallel}^A is frequency independent. Here $\epsilon_{\perp}^A(\infty)$ is a measure of the influence of the electronic polarizability on the dielectric response of the structure.

The dipole selection rule introduced some years ago¹⁴ concludes that, in the near-specular dipole spectrum, only vibrations that generate an oscillatory electric dipole moment perpendicular to the surface are observable. We have tested this rule in the present instance, for the model described below, by introducing vibrational resonances into $\epsilon_{\parallel}^A(\omega)$. We find no hint of vibrational structure in the loss spectrum when this is done. We conclude that the modes observed in the spectrum then indeed have symmetry such that the associated dynamic dipole moment is normal to the surface.

Our studies of the vibrational losses use $d = d_A + d_B = 15.4 \text{ \AA}$ for the combined thickness of the A and B layers. We use 3.1 \AA for the thickness d_B of the highly conducting CuO_2 sheets (there are two in this material). These are compatible with structural studies of the Bi 2:2:1:2 materials.¹⁵ We assume that upon cleavage the crystal splits between the two BiO planes. This places the thickness of the outer C layer at 4.6 \AA .

In addition to the oscillator strengths, frequencies, and widths of the vibrational resonances, we also require the electronic contributions $\epsilon_{\perp}^A(\infty)$, $\epsilon_{\parallel}^A(\infty)$ to the dielectric response of the A layers, and similarly for the B layers. The conductivity of the B layers is so high that the calculated loss spectra are quite insensitive to the choice of $\epsilon_{\parallel}^B(\infty)$, for any reasonable value of this parameter. We choose $\epsilon_{\perp}^A(\infty)$ and $\epsilon_{\parallel}^B(\infty)$ so that we reproduce the measured infrared reflectivities for frequencies well above the vibrational-resonances region,⁷ using the scheme outlined below.

In Fig. 4(a), we show an energy-loss spectrum calculated as just described. It has been assumed here that the outermost C layer has dielectric response characteristics identical to the interior A layers, though the C layer is thinner as mentioned above. We have used $\epsilon_{\perp}^B(\infty) = 8$, $\epsilon_{\parallel}^A(\infty) = 4.5$, and $\epsilon_{\parallel}^B(\infty) = 4$; the calculated spectra are influenced only modestly by changes in $\epsilon_{\parallel}^A(\infty)$, and this parameter does not enter our description of the ir reflectivity. The resistivity ρ_0 of the material in the conducting layers of $106 \mu\Omega$ cm produces an acceptable background intensity in the 100-meV region. The oscillator strengths and other vibrational parameters are summarized in Table I.

The parameters above are most reasonable, from a physical point of view. One may inquire about their uniqueness.

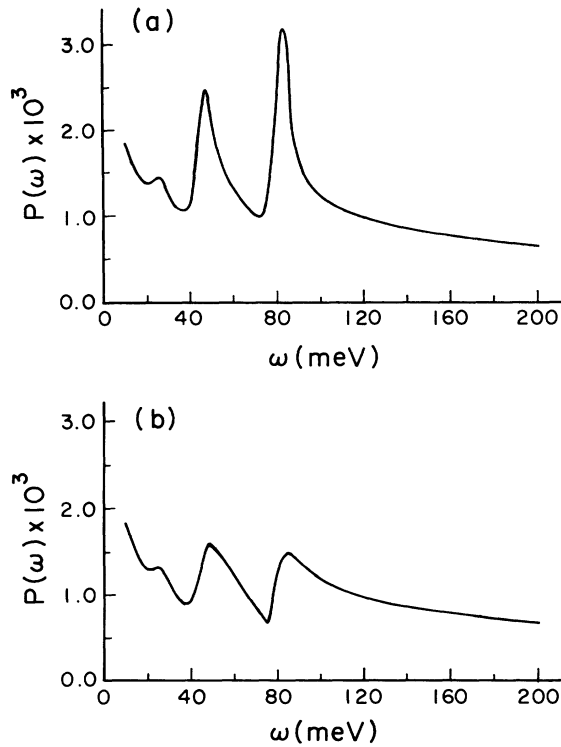


FIG. 4. (a) The electron loss function $P(\omega)$, calculated for the model described in the text. In this case, the outer C layer is a vibrationally active insulator. (b) The electron loss function $P(\omega)$, calculated for the case where the C layer contains no dipole-active vibrations. The vibrationally active layers thus lie below the outermost conducting layer.

We believe the value inferred for the resistivity of the conducting layers to be reasonably secure. The calculated background near and above 100 meV is rather insensitive to the vibrational parameters, and various other microscopic details.

There are, however, ambiguities in the remaining parameters. For example, if one considers an isolated, thin dielectric film with a dipole-active vibrational resonance perpendicular to the surface, one may see that the strength of the vibrational loss in the near-specular electron loss cross section scales as $[A/\epsilon_1(\infty)]^2$. Thus it is difficult to determine A and $\epsilon_1(\infty)$ uniquely from the mode intensity in the electron loss spectrum alone. We have constrained $\epsilon_1^A(\infty)$ and $\epsilon_1^B(\infty)$ through contact with infrared reflectivity data, as discussed below. But we could have chosen $\epsilon_1^B(\infty)$ somewhat smaller, and $\epsilon_1^A(\infty)$ somewhat larger, and increased the oscillator strengths A_j upward, to still find a satisfactory account of both data sets. In the end, we have a model which provides a

TABLE I. Vibrational parameters used to generate the loss spectra displayed in Fig. 4.

j	ω_j (meV)	γ_j (meV)	A_j (meV)
1	21.8	8	40
2	36	8	70
3	72	7	75

very good account of the electron loss data, and, we shall see, the reflectivity in the infrared. This allows us to conclude firmly that the electron loss data are recording the spectrum intrinsic to the material. But care must be exercised if, for example, one wishes to link our parameters to microscopic theories of these materials, because there are ambiguities in the choices, as just discussed.

The theoretical spectrum in Fig. 4(a) assumes the C layer, which lies outside the first conducting CuO_2 layer, is vibrationally active with dipole resonances identical to those of the insulating A layers in the crystal interior. One can inquire how the loss spectrum would appear if the conducting layer were the outermost. We illustrate this in Fig. 4(b), where we suppress the contribution from the vibrational resonances in the C layer. The loss spectrum has changed dramatically. In essence, in Fig. 4(b), we see a free-carrier background, modulated by the vibrational resonances in the underlying material. We have been unable to produce anything close to the experimental spectrum with the conducting layer outermost. We argue the electron loss data provide strong evidence that the outermost layer is insulating.

We turn next to the infrared data. Our interest lies in data reported by Zibold *et al.*,⁷ where the infrared reflectivity is measured in a geometry where the electric field is perpendicular to the surfaces of the constituents of the layered structure. The data are reported in their Figs. 5 and 6. These authors analyze the data by assuming the material to be described by a simple frequency-dependent dielectric function. We argue one should recognize the multilayer character of the medium, and utilize effective-medium theory to synthesize an effective dielectric response function $\bar{\epsilon}_1(\omega)$ from that of the individual constituents. One finds, after a simple analysis,¹⁶ that for this geometry

$$\bar{\epsilon}_1(\omega) = \frac{\epsilon_1^A(\omega)\epsilon_1^B(\omega)}{f_B\epsilon_1^A(\omega) + f_A\epsilon_1^B(\omega)}. \quad (14)$$

We show the infrared reflectivity calculated from our model in Fig. 5. Our theory is presented as a dotted line. We also reproduce in the figure the reflectivity data of Zibold *et al.*, given as a solid line. Note that the data do not extend below 40 meV. Thus, Zibold *et al.* did not observe the rather weak, low-frequency mode observed in the electron loss spectrum. The agreement between our Fig. 5, and the reflectivity data is very good indeed, with one exception. Zibold *et al.* observe two vibrational resonances in the 30–40 meV region, while only a single feature appears in the electron loss data. The discrepancy may have its origin in the limited resolution of the electron loss method. We note, for example, that the loss peak in the 45 meV region of Fig. 1 is somewhat broader than the other two structures, so improved resolution may show that two modes in fact contribute to this feature.

IV. GENERAL DISCUSSION AND CONCLUSIONS

We have presented the theory of near-specular dipole scattering of electrons from the surface of a layered ma-

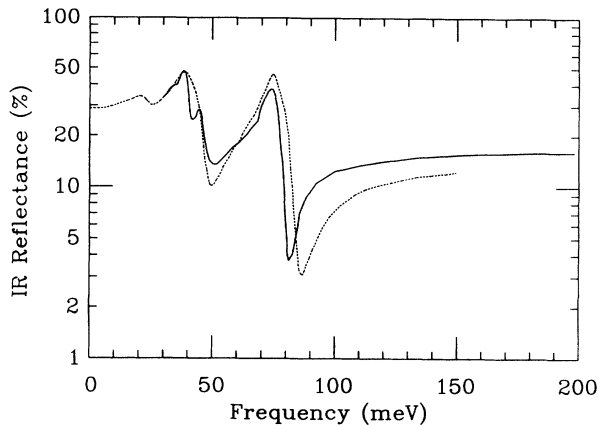


FIG. 5. The infrared reflectivity, calculated using effective-medium theory, for the model used to generate Fig. 4. The calculated reflectivity is shown as a dotted line. The solid line is the reflectivity data reproduced from Ref. 7.

material, such as the superconducting cuprates. The analysis extends earlier descriptions^{8,9} of such structures to incorporate the anisotropic nature of the constituents of these materials.

We have applied the theory to a quantitative description of electron loss data from Bi 2:2:1:2 compounds reported in Ref. 5, to obtain a picture compatible with the infrared reflectivity data reported by Zibold *et al.*,⁷ though evidently one mode is not resolved in the electron loss studies. This analysis allows us to conclude that the experiments in Ref. 5 indeed yield the intrinsic electron loss spectrum, for a material whose outermost layer is a vibrationally active ionic insulator.

The data in Ref. 5 have a background higher than that reported by Lieber and his collaborators by two to three orders of magnitude. Our analysis of these high-background data yields a value for the resistivity of the CuO₂ layers, 106 $\mu\Omega$ cm, that we believe quite reasonable. We have inquired if we can use model parameters to reproduce the very low backgrounds reported by Lieber and co-workers,⁴ but we have been unable to do this. For instance, even if we assign to the CuO₂ layers a conductivity equal to that of room-temperature Cu, the background at 100 meV only drops by about an order of magnitude, to 1.4×10^{-4} , which is still very much higher than that reported by Lieber and his collaborators. Our inability to obtain an account of these low backgrounds with reasonable material parameters strongly reinforces the arguments advanced in Ref. 5 that the data reported by Lieber *et al.* were taken under conditions where surface charging is present.

We saw in Sec. II that the high backgrounds found for the high- T_c materials have their origin, in part, in the anisotropic nature of the conductivity in these materials. We have calculated $P(\omega)$ at 100 meV for copper metal at room temperature, to find $P(\omega) = 6 \times 10^{-6}$ meV⁻¹, a value far smaller than the 1.4×10^{-4} meV⁻¹ quoted in the previous paragraph for the layered materials with conductivity equal to copper, but only parallel to the surface. Data reported some years ago indeed show such a very small background for Cu metal.¹⁷

We next comment on the physical nature of the loss peaks which appear in the electron loss spectrum. First, recall the nature of the loss peaks observed on the surface of a simple ionic material, with an infrared-active optical phonon in its bulk. The peak in the infrared absorptivity is controlled by $\text{Im}[\epsilon(\omega)]$, with $\epsilon(\omega)$ the dielectric constant. The peak in the infrared absorption occurs at the transverse optical phonon frequency, ω_{TO} . The peaks in the electron loss spectrum occur above ω_{TO} , at the frequency ω_s of a surface optical phonon referred to frequently as the Fuchs-Kliwer mode.^{2,3} One has $\omega_s > \omega_{\text{TO}}$. In fact,

$$\omega_s [(\epsilon_s + 1)/(\epsilon_\infty + 1)]^{1/2} \omega_{\text{TO}},$$

where ϵ_s and ϵ_∞ are the static and high-frequency dielectric constants, respectively.

The anisotropic, layered structure modeled here also has surface collective modes that are the analog of the Fuchs-Kliwer modes. Unfortunately, these are not described by elementary formulas, but occur as poles in the (ω, Q_{\parallel}) plane of the loss function $R(Q_{\parallel}, \omega)$. These collective modes are damped, in our model, by virtue of the dissipation in the conducting layers described by the finite relaxation time $\tau(\omega)$. One may appreciate the fact that we have surface collective modes in our theoretical energy loss spectrum by comparing the location of the loss peaks in Fig. 4(a) with those in Fig. 5. For the high-frequency mode, the peak in our model of $\text{Im}[\bar{\epsilon}(\omega)]$ occurs at 68 meV, while the corresponding feature in the electron loss spectrum is upshifted to 80 meV.

While the experimental spectra were taken at the temperature of 47 K, well below the superconducting transition, there is no evidence of a superconducting gap in the data. There are several possibilities for the absence of such a structure. First, the gap feature would reside within the “phonon forest” evident in Fig. 2, and thus just may be difficult to extract from the full data. It is also possible that these samples are not superconducting in the near vicinity of their surface. However, photoemission experiments have detected the energy gap, and these experiments study electrons whose mean free path is only a few angstroms. Moreover, recent infrared results for both Bi 2:2:1:2 (Ref. 18) YBa₂Cu₃O₇ (Ref. 19) have demonstrated that the optical conductivity is gapless in the *bulk* of these materials. Hence there is a strong evidence which suggests that the surface properties deduced from our electron-energy-loss data reflect the intrinsic properties of high- T_c materials in their superconducting state.

It is possible that the nature of the superconducting state in these materials is such that the structure in $\sigma_{\parallel}(\omega)$ is more subtle than expected for an isotropic s -wave state where, as discussed by Persson and Demuth,⁴ there should be a strong signature in the electronic background (provided this is not obscured by a strong phonon loss). If, however, the pairing is of d -wave character, the energy gap has zeros on the Fermi surface, and is thus very anisotropic. Very likely the structure in $\sigma_{\parallel}(\omega)$ would then be much less pronounced than for the isotropic s -

wave case. Similar remarks may apply to *s*-wave pairing models which yield a highly anisotropic gap. The absence of structure in $\sigma_{\parallel}(\omega)$ may then be evidence, albeit indirect, for a pairing scenario that leads to a highly anisotropic gap. It would be of great interest to see explicit calculations of $\sigma_{\parallel}(\omega)$ for such models of the cuprate superconductors.

ACKNOWLEDGMENTS

The research of D.L.M. was supported by the Department of Energy, through Grant No. DE-FG03-84ER45083, while that of R.B.P. and L.L.K. was supported by the Department of Energy through Grant No. DE-FG02-84ER45147.

¹For example, see L. H. Dubois, G. P. Swartz, R. E. Camley, and D. L. Mills, *Phys. Rev. B* **29**, 3208 (1984); B. N. J. Persson and J. E. Demuth, *ibid.* **30**, 5968 (1984); H. Lüth, *Surf. Sci.* **168**, 773 (1986).

²D. L. Mills, *Surf. Sci.* **48**, 59 (1975).

³H. Froitzheim, H. Ibach, and D. L. Mills, *Phys. Rev. B* **11**, 4980 (1975); also H. Ibach and D. L. Mills, *Electron Energy Loss Spectroscopy and Surface Vibrations* (Academic, San Francisco, 1982), Chap. 3. We wish to call the reader's attention to the discussion of multiple scattering effects by Persson and Demuth in the paper cited in Ref. 1.

⁴J. E. Demuth, B. N. J. Persson, F. Holtzberg, and C. V. Chandrasekhar, *Phys. Rev. Lett.* **64**, 603 (1990); B. N. J. Persson and J. E. Demuth, *Phys. Rev. B* **42**, 8057 (1990); Y. Li, J. L. Huang, and C. M. Lieber, *Phys. Rev. Lett.* **68**, 3240 (1992); Y. Li, J. Liu, and C. M. Lieber, *ibid.* **70**, 3494 (1993).

⁵R. B. Phelps, P. Akavoor, L. L. Kesmodel, A. L. Barr, J. T. Markert, J. Ma, R. J. Kelley, and M. Onellion, this issue, *Phys. Rev. B* **50**, 6526 (1994).

⁶R. Franchy, B. Decker, J. Masuch, and H. Ibach, *Surf. Sci.* **55**, 303 (1994).

⁷A. Zibold, M. Dürrieler, A. Gaymann, H. P. Geserich, N.

Nücker, V. M. Burlakov, and P. Müller, *Physica C* **193**, 171 (1992).

⁸R. E. Camley and D. L. Mills, *Phys. Rev. B* **29**, 1695 (1984).

⁹S. R. Streight and D. L. Mills, *Phys. Rev. B* **35**, 6337 (1987).

¹⁰Burl M. Hall and D. L. Mills, *Phys. Rev. B* **44**, 1202 (1991).

¹¹For example, see Fig. 3 of the paper by Li, Liu, and Lieber cited in Ref. 4, and the associated discussion.

¹²See H. Ibach and D. L. Mills in Ref. 3.

¹³B. C. Webb, A. J. Sievers, and T. Mihalisin, *Phys. Rev. Lett.* **57**, 1951 (1986).

¹⁴E. Evans and D. L. Mills, *Phys. Rev. B* **5**, 4126 (1972).

¹⁵C. C. Toradi, J. B. Parise, M. A. Subramanian, J. Gopalakrishnan, and A. W. Sleight, *Physica C* **157**, 115 (1989).

¹⁶V. Agranovich and V. E. Kratsov, *Solid State Commun.* **55**, 373 (1985).

¹⁷S. Anderson and B. N. J. Persson, *Phys. Rev. Lett.* **50**, 2028 (1983).

¹⁸D. Mandrus, M. C. Martin, C. Kendziora, D. Koller, L. Forro, and L. Mihaly, *Phys. Rev. Lett.* **70**, 2629 (1993).

¹⁹M. J. Sumner, J. T. Kim, and T. R. Lemberger, *Phys. Rev. B* **47**, 12248 (1993).